Electrically pumped ultraviolet ZnO diode lasers on Si

Sheng Chu, Mario Olmedo, Zheng Yang, Jieying Kong, and Jianlin Liu[a)]
Quantum Structures Laboratory, Department of Electrical Engineering, University of California at Riverside, Riverside, California 92521, USA

(Received 27 August 2008; accepted 10 October 2008; published online 4 November 2008)

Electrically pumped ZnO quantum well diode lasers are reported. Sb-doped *p*-type ZnO/Ga-doped *n*-type ZnO with an MgZnO/ZnO/MgZnO quantum well embedded in the junction was grown on Si by molecular beam epitaxy. The diodes emit lasing at room temperature with a very low threshold injection current density of 10 A/cm^2. The lasing mechanism is exciton-related recombination and the feedback is provided by close-loop scattering from closely packed nanocolumnar ZnO grains formed on Si. © *2008 American Institute of Physics*. [DOI: 10.1063/1.3012579]

Owing to the large exciton binding energy in ZnO, exciton-exciton scattering induced stimulated emission is readily achieved in experimental demonstrations. ZnO lasing has been mostly achieved by optically pumping disordered particles (random lasers),[1,2] nanowires (nanowire lasers),[3,4] hexagonal nanonails (whispering gallery mode lasers),[5] and thin films.[6–8] Recently, electrically pumped random lasing was further realized based on ZnO/dissimilar material heterojunction diodes[9] and ZnO based metal oxide semiconductor devices.[10] Obviously the creation of random laser diode based on ZnO *p-n* junction with high light gain is critical toward future ultraviolet laser application. However, the difficulty in the development of electrically pumped ZnO *p-n* junction devices is primarily due to the lack of reliable and controllable *p*-type ZnO. Previously we reported reliable antimony (Sb)-doped *p*-type ZnO.[11,12] We also developed various ultraviolet optoelectronic devices such as photodetectors[13] and light emitting diodes.[14,15] Here we report the electrically pumped efficient ZnO ultraviolet diode lasers on Si.

ZnO junction lasers were grown on *n*-type Si (100) substrate (1–20 Ω cm) using molecular beam epitaxy system. The device scheme is shown in Fig. 1(a). A thin magnesium oxide (MgO) buffer layer was deposited at 350 °C to reduce the lattice mismatch between Si and ZnO, which was followed by the growth of a thin ZnO buffer layer of about 15 nm at the same substrate temperature. On top of this thin buffer, ZnO *p-n* junction structure was formed. The *n*-type and *p*-type ZnO layer was formed by Ga doping at 450 °C and Sb doping at 550 °C, respectively. The thickness of both *n*-type and *p*-type layers is 340 nm. In between *p*-type layer and *n*-type layer, a single ZnO quantum well with thickness of about 1 nm was deposited by using a wider bandgap MgZnO of about 1.5 nm as barrier. The mole fraction of Mg is about 0.1, leading to a conduction band offset between ZnO and MgZnO of about 0.21 eV.[16] Optical lithography and wet etching were used to define square-shape mesa diode devices of 500×500 μm^2. Au/NiO (500/30 nm) and Au/Ti (200/30 nm) were then deposited on *p*-type ZnO and *n*-type ZnO, respectively, by lift-off process and properly annealed to form Ohmic contacts.

X-ray diffraction (XRD) $\theta/2\theta$ scans suggest that the diode film grows preferentially along the *c*-direction of the ZnO wurtzite lattice [Fig. 1(b)]. Scanning electron microscopy (SEM) images in Figs. 1(c) and 1(d) show the top view and the side view of the ZnO film on Si substrate. The images reveal that vertical ZnO nanocolumnar structures are formed, which are the typical result of oriented nucleation process as a result of the large lattice mismatch between ZnO and Si substrate.[17] The in-plane size of the columnar grains ranges from 100 to 400 nm. The grains are packed closely to form a continuous "thin film." Figure 1(e) schematically shows detailed structure of the ZnO diode laser.

After Au/NiO to *p*-type ZnO and Au/Ti to *n*-type ZnO Ohmic contacts were formed, electrical properties of the diodes were characterized by Agilent B 1500 A semiconductor parameter analyzer and 4284A *LCR* meter. Figure 2 shows the current-voltage characteristics of one typical ZnO laser device (the left inset is its linear version), suggesting typical diode rectifying characteristics. The result (right inset) is the capacitance-voltage characteristics of the diode showing diode linear characteristic with a reasonable built-in potential of about 3.14 V.

The laser diode was biased at room temperature under dc forward voltages; in other words, continuous current injection mode was used to obtain lasing. The lasing was collected from the sample surface. Under low injection current of 10 mA, weak spontaneous emission band centered at around 378 nm was observed, as shown in Fig. 3(a). This peak is attributed to free exciton spontaneous emission. As the injection current increases to about 20 mA, dramatic sharp emissions with a line width as narrow as 0.4 nm emerge from the single-broad emission spectra around 380 nm, which indicates that the gain is now large enough to enable cavity mode to start lasing. Further increase in the injection current from 20 to 60 mA increases both the number and the intensity of sharp lasing mode peaks in the spectral region between 360 and 400 nm, as shown in Fig. 3(b). The center of the lasing spectrum redshifts about 4–5 nm as the drive current increases from 10 to 60 mA, which is due to temperature-induced bandgap variations.

Figure 4 shows the plot of the integrated lasing spectrum intensity and laser output power as a function of injection current. The output power was measured using a Thorlab PM 120 V power meter. The integrated lasing spectrum intensity matches reasonably well with the output power data trend. A

a)Author to whom correspondence should be addressed. Electronic mail: jianlin@ee.ucr.edu.

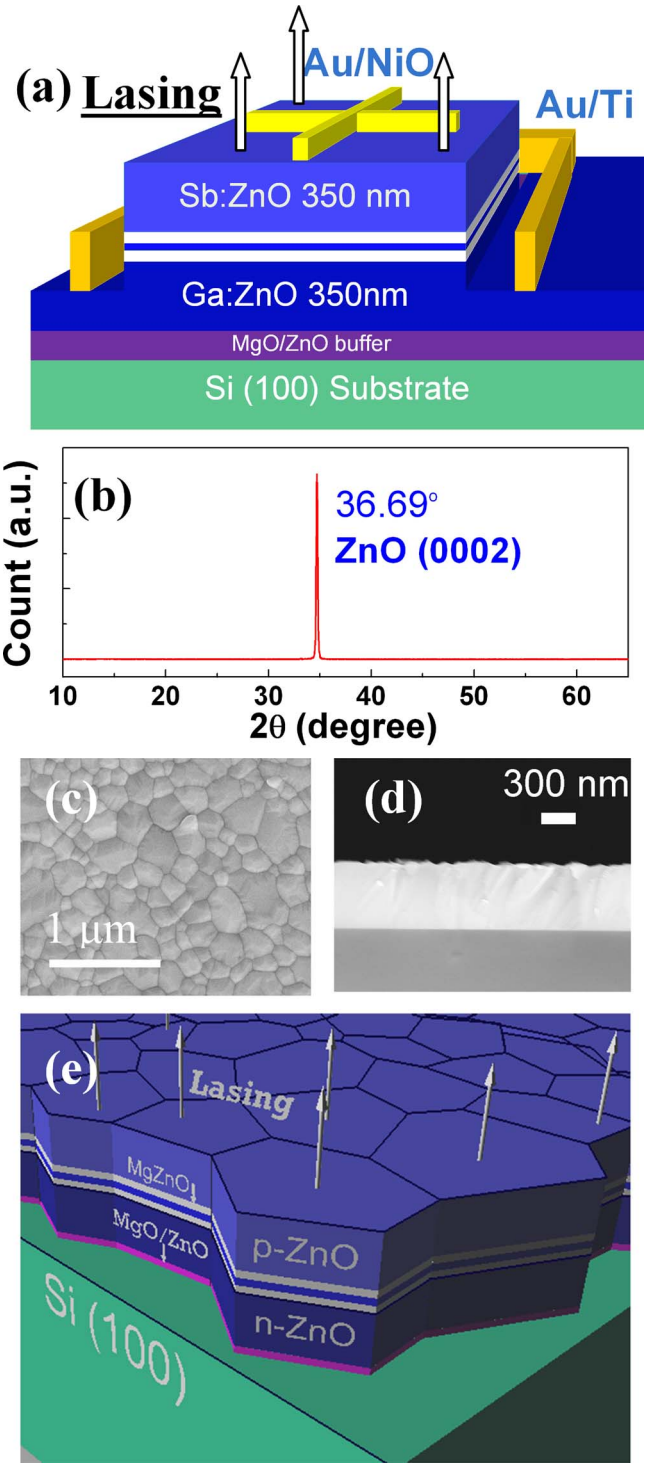

FIG. 1. (Color online) (a) Schematic of the ZnO laser diode showing a single quantum well sandwiched between *p*-type and *n*-type layers. Device mesa with Au/NiO and Au/Ti Ohmic contacts is also shown. (b) XRD θ-2θ scan of the laser sample. The result suggests that ZnO preferentially grows along (0001) direction of the ZnO wurtzite lattice. (c) SEM image of sample surface. (d) Cross-sectional SEM image of the ZnO diode. (e) Schematic of the columnar structures of the ZnO diode "film" on Si substrate.

solid line is plotted to guide the eyes, showing the threshold current of about 25 mA, corresponding to current density of 10 A/cm^2. The output power is about 0.5 μW at 60 mA drive current. Further increase in driving current beyond 60 mA leads to sharper increase in output power, a deviation of the trend suggested by the solid line, for example, 1.4 μW at 80 mA and 11.3 μW at 130 mA. This is an indication of

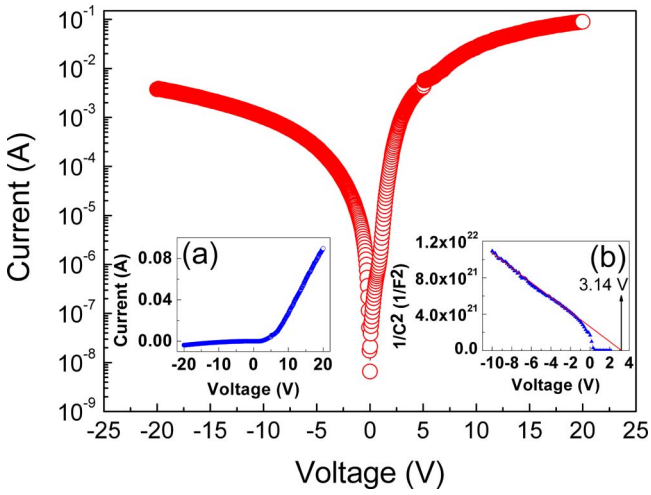

FIG. 2. (Color online) *I-V* characteristics in semilogarithmic scale of the laser diode showing typical rectifying characteristics. The left inset (a) shows the *I-V* curve in linear scale, while the right inset (b) shows *C-V* characteristics further confirming *p-n* junction with built-in potential of about 3.14 V.

exciton lasing.[18] The very low turn-on current mainly results from strong exciton recombination efficiency from localization effect in the quantum well.

So what is the reason behind the strong lasing from the surface of the ZnO diodes? First ZnO nanowire can es-

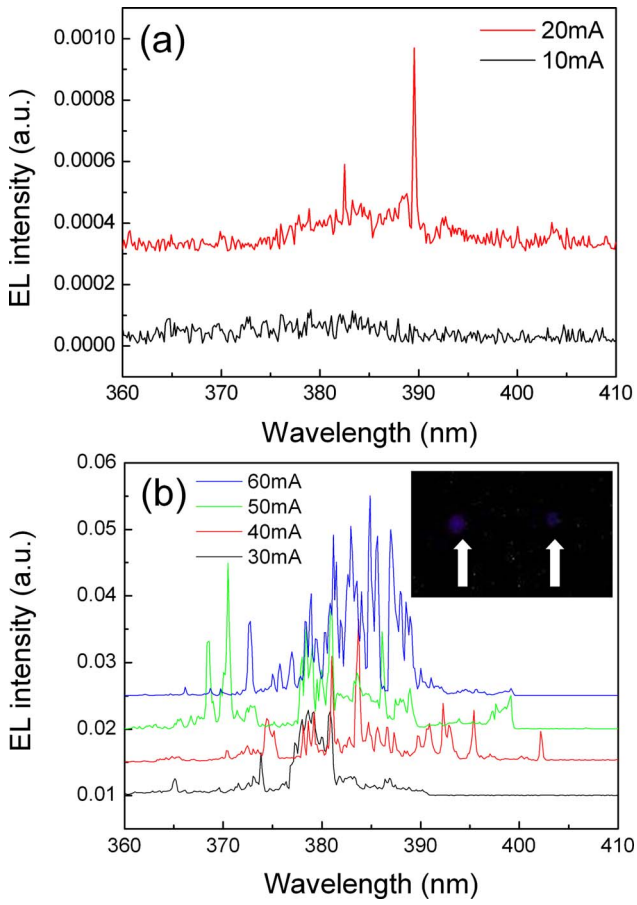

FIG. 3. (Color online) (a) EL spectra with low injection currents of 10 and 20 mA. Lasing effect is evident when the injection current reaches about 20 mA. (b) EL spectra with higher injection currents from 30 to 60 mA. All spectra are within UV around 380 nm. The spectra were shifted in *y* scale for clarity. Inset is an optical microscope image of lasing device driven at 30 mA. Arrows indicate isolated lasing spots on the diode surface.

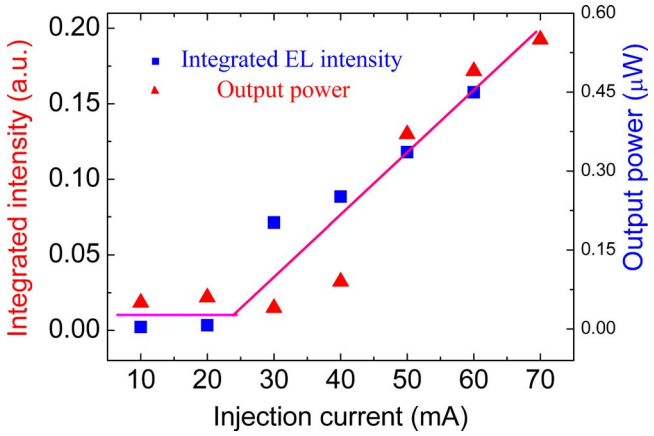

FIG. 4. (Color online) Integrated EL intensity and output power as a function of the injection current. Threshold current can be determined to be about 25 mA. The output power is 0.5 μW at 60 mA.

tablish Fabry–Pérot (FP)-type resonant cavity by two end facets of the nanowire in the optical pumping scheme.[3] However, the length of the nanowirelike grains here is 700 nm, which is too small to provide sufficient gain to overcome loss. According to the FP laser theory, the threshold gain g is inversely proportional to the gain length L: $g = L^{-1} \ln(R_{\text{top}} R_{\text{bottom}})$, where in our case L is the grain thickness, R_{top} is the reflectivity between ZnO and air, and R_{bottom} is the reflectivity between ZnO and Si. A simple calculation gives required threshold gain of at least 12.8×10^3 cm^{-1}. This number is too large. In other words, the single grain resonant cavity with two end facets cannot provide enough feedback in this case. Secondly, polariton related laser can exhibit ultralow threshold[19] with the wavelength of emissions comparable with the size of the cavity, and polariton modes have been reported in ZnO nanowires.[20] However, in our case there is no evidence of polariton existence even in low temperature photoluminescence spectra (not shown here); therefore, we may safely exclude this possibility. Here we tentatively believe that light scattering from the grain boundaries may form close loops to establish gain, i.e., random lasing may be the reason for lasing. A signature of random lasing is that the light emits in all directions. Our devices show similar lasing spectra at 0–60° with respect to the normal direction (not shown here). This is reasonable since the side walls of each grain are not strictly perpendicular to the substrate; thus light can be scattered in all directions. The UV light generated by the diode undergoes scattering at the grain boundaries. When the scattering is strong enough and the mean free path of the light is comparable to its wavelength, then some of the light can be scattered in their original places. As a result, close-loop resonant cavities for coherent lasing are formed. When the generation rate of light overcomes the lost, lasing oscillation behavior dominates over the electroluminescence (EL) spectra. Furthermore, the lasing effect can be verified by images from optical microscope. Dotted patterns in the inset of Fig. 3(b) represent the isolated random resonators at the injection current of 30 mA.

As long as the randomly formed close-loop resonant cavities are possible, carrier population inversion is another critical condition required for lasing in diode lasers. In our diode, the lasing is related to exciton emissions closely associated with the embedded MgZnO/ZnO/MgZnO quantum well. It should be noted that the devices without the quantum well structures do not exhibit lasing actions.[21] As the diode is forward biased, the injected electrons and holes quickly form excitons and become localized around the quantum well. More carriers injected into the junction at the higher drive currents result in exciton-exciton inelastic collisions, which dissociate the localized excitons to form carrier population inversion conditions for stimulated emissions.

In conclusion, we realized electrically pumped ZnO diode lasers on Si using Sb-doped ZnO as p-type layer and Ga-doped ZnO as n-type layer with a MgZnO/ZnO/MgZnO quantum well in between. Ultraviolet lasing at around 380 nm was demonstrated at room temperature with very low lasing threshold current density of 10 A/cm^2. The output power of this laser was measured to be 11.3 μW at 130 mA driving current. This work has experimentally proven electrically pumped ZnO exciton ultraviolet lasing, which may find potential applications.

This work was supported by the DMEA through the Center for NanoScience and Innovation for Defense (CNID) under Award No. H94003-07-2-0703 and ARO-YIP award.

[1] H. Cao, Y. G. Zhao, H. C. Ong, S. T. Ho, J. Y. Dai, J. Y. Wu, and R. P. Chang, Appl. Phys. Lett. **73**, 3656 (1998).
[2] S. F. Yu, C. Yuan, S. P. Lau, W. I. Park, and G. Yi, Appl. Phys. Lett. **84**, 3241 (2004).
[3] M. H. Huang, S. Mao, H. Feick, H. Q. Yan, Y. Y. Wu, H. Kind, E. Weber, R. Russo, and P. D. Yang, Science **292**, 1897 (2001).
[4] L. K. van Vugt, S. Rühle, and D. Vanmaekelbergh, Nano Lett. **6**, 2707 (2006).
[5] D. Wang, H. W. Seo, C.-C. Tin, M. J. Bozack, J. R. Williams, M. Park, and Y. Tzeng, J. Appl. Phys. **99**, 093112 (2006).
[6] Z. K. Tang, G. K. L. Wong, P. Yu, M. Kawasaki, A. Ohtomo, H. Koinuma, and Y. Segawa, Appl. Phys. Lett. **72**, 3270 (1998).
[7] D. M. Bagnall, Y. F. Chen, Z. Zhu, T. Yao, S. Koyama, M. Y. Shen, and T. Goto, Appl. Phys. Lett. **70**, 2230 (1997).
[8] Y. R. Ryu, J. A. Lubguban, T. S. Lee, H. W. White, T. S. Jeong, C. J. Youn, and B. J. Kim, Appl. Phys. Lett. **90**, 131115 (2007).
[9] E. S. P. Leong and S. F. Yu, Adv. Mater. (Weinheim, Ger.) **18**, 1685 (2006).
[10] X. Ma, P. Chen, D. Li, Y. Zhang, and D. Yang, Appl. Phys. Lett. **91**, 251109 (2007).
[11] F. X. Xiu, Z. Yang, L. J. Mandalapu, D. T. Zhao, J. L. Liu, and W. P. Beyermann, Appl. Phys. Lett. **87**, 152101 (2005).
[12] F. X. Xiu, Z. Yang, L. J. Mandalapu, D. T. Zhao, and J. L. Liu, Appl. Phys. Lett. **87**, 252102 (2005).
[13] L. J. Mandalapu, Z. Yang, F. X. Xiu, D. T. Zhao, and J. L. Liu, Appl. Phys. Lett. **88**, 092103 (2006).
[14] L. J. Mandalapu, Z. Yang, S. Chu, and J. L. Liu, Appl. Phys. Lett. **92**, 122101 (2008).
[15] S. Chu, L. J. Mandalapu, Z. Yang, and J. L. Liu, Appl. Phys. Lett. **92**, 152103 (2008).
[16] N. B. Chen and C. H. Sui, Mater. Sci. Eng., B **126**, 16 (2006).
[17] J. W. Shin, J. Y. Lee, Y. S. No, T. W. Kim, and W. K. Choi, J. Appl. Phys. **100**, 013526 (2006).
[18] D. M. Bagnall, Y. F. Chen, Z. Zhu, T. Yao, M. Y. Shen, and T. Goto, Appl. Phys. Lett. **73**, 1038 (1998).
[19] M. Zamfirescu, A. Kavokin, B. Gil, G. Malpuech, and M. Kaliteevski, Phys. Rev. B **65**, 161205 (2002).
[20] S. Ruhle, L. K. van Vugt, H. Y. Li, N. A. Keizer, L. Kuipers, and D. Vanmaekelbergh, Nano Lett. **8**, 119 (2008).
[21] J. Y. Kong, S. Chu, M. Olmedo, Z. Yang, and J. L. Liu, Appl. Phys. Lett. **93**, 132113 (2008).